DOI: 10.1002/asia.200700112

Experimental and Theoretical Investigations into the Paratropic Ring Current of a Porphyrin Sheet

Yasuyuki Nakamura, Naoki Aratani, and Atsuhiro Osuka*[a]

Abstract: Anomalous induced magnetic effects were observed in a directly fused square-planar porphyrin sheet **1**, in that the protons above the center of the tetraporphyrin core were characteristically shifted downfield in the ^{1}H NMR spectrum. These observations suggest a rare paratropic ring-current effect around the planar cyclooctatetraene (COT) core of **1**. To examine the spatial distribution of the induced magnetic effect, face-to-face dimeric complexes of porphyrin sheet **1** with bipyridyl-type guest molecules (**G1**–**G3**) were prepared, which provided complexation-induced shifts (CISs) of the guest molecules as a neat experimental guide to the distance dependence of the induced magnetic effects in **1**. Nucleus-independent chemical shift (NICS) values of **1** were calculated by varying the distance of the probe from the plane of **1**. Whereas a simple bell-type profile was estimated for the complex $(\mathbf{1})_2$–$(\mathbf{G1})_4$, the distance profiles of the CIS became increasingly flat for $(\mathbf{1})_2$–$(\mathbf{G2})_4$ and $(\mathbf{1})_2$–$(\mathbf{G3})_4$. Finally, we investigated the paratropic ring-current effect just above the COT core of the complex **1**–$(\mathbf{G4})_2$, which agrees well with the theoretically estimated distance-dependent induced magnetic effect. Consequently, both experimental and theoretical studies on the complexes of porphyrin sheets with guest molecules revealed for the first time a unique distance dependence of the paratropic ring current.

Keywords: conjugation · host–guest systems · macrocycles · paratropic ring current · porphyrinoids

Introduction

^{1}H NMR chemical shifts are a fundamentally important source of information for the complexation of organic molecules and biomolecules in solution.[1] A number of investigations and several technological improvements have established ^{1}H NMR spectroscopy as a standard tool for protein-structure determination.[2,3] The heme ring plays an important role in improving the quality of the final structure obtained, as the presence of an aromatic ring causes large changes in the chemical shifts of nearby residues. This effect, the so-called "ring current", is strongly associated with the aromatic character of a system. The aromaticity of porphyrins has traditionally been rationalized as a consequence of an 18-π-electron circuit that can be drawn in their valence-bond structure.[4] The strong magnetic effect of the aromatic ring current of porphyrins is also useful in coordination chemistry, in that the ^{1}H NMR signals of the protons of bound molecules above the porphyrin ring are characteristically shifted upfield. Coordination of pyridine derivatives toward zinc(II) porphyrin has frequently been used for the construction of various functional supramolecular systems, in which the protons of bound pyridine are largely shielded.[5] The distance dependence of such magnetic effects is quite important for determining the actual placement of a guest proton with regard to the porphyrin host as well as for understanding the aromatic electronic properties. Thus, both experimental and theoretical studies on the distance dependence of magnetic effects have been performed for the diatropic ring current of porphyrins. Induced magnetic effects of porphyrins were extensively examined by Abraham et al. by ^{1}H NMR spectroscopy.[6] On the other hand, there are only a few experimental studies on the paratropic ring current because of very limited examples of suitable stable antiaromatic molecules.[7]

Recently, we reported the synthesis of directly fused square-planar porphyrin sheet **1** (Scheme 1), which shows anomalous induced magnetic effects.[8] Curiously, the ^{1}H NMR signals of the 1,4-phenylene protons in the 1:2

[a] Y. Nakamura, Dr. N. Aratani, Prof. Dr. A. Osuka
Department of Chemistry
Graduate School of Science
Kyoto University
Sakyo-ku, Kyoto 606-8502 (Japan)
Fax: (+81) 75-753-3970
E-mail: osuka@kuchem.kyoto-u.ac.jp

Supporting information for this article is available on the WWW under http://www.chemasianj.org or from the author.

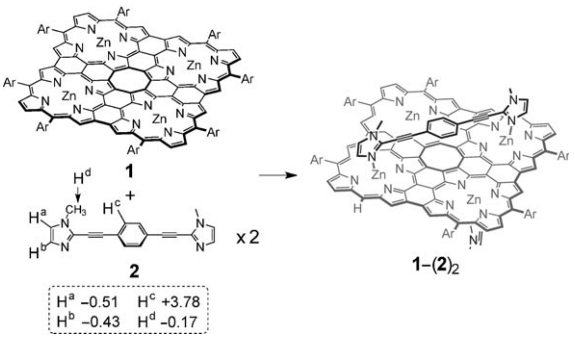

Scheme 1. Formation of the complex of **1** and **2**, and the complexation-induced shifts (CISs) in ppm (see text). Ar = 3,5-di-*tert*-butylphenyl.

complex, defined as type I complex **1**–(**2**)$_2$, were shifted downfield by 3.78 ppm. This anomalous shift was interpreted in terms of a paratropic ring-current effect around the cyclooctatetraene (COT) core of **1**, which is forced to be planar owing to the multiply fused porphyrins.

In this paper, we report the effective formation of type II (2:4 sandwich) complexes (**1**)$_2$–(**G1**)$_4$, (**1**)$_2$–(**G2**)$_4$, and (**1**)$_2$–(**G3**)$_4$, as well as a further example of a type I complex, **1**–(**G4**)$_2$, in $CDCl_3$ (Scheme 2). Examination of the ^{1}H NMR spectra of these complexes provided useful information on the distance dependence of the magnetic effects of **1**. These magnetic effects are also examined theoretically.

Results and Discussion

Synthesis

Porphyrin sheet **1** was prepared from a directly *meso*,*meso*-linked cyclic porphyrin tetramer.[8] The inherent poor solubility of **1** was improved by the addition of *n*-butylamine; this procedure is quite important for manipulations such as separation, final purification, and ^{1}H NMR spectroscopy. Compounds **G2** and **G3** were synthesized by palladium-catalyzed coupling of (4-pyridyl)boronic acid pinacol ester with 1,4-dibromobenzene and 4,4′-dibromobiphenyl, respectively.[9] **G4** was synthesized by following the published procedure.[10]

Experimental Studies

The complexation behavior of **1** with **G1**, **G2**, and **G3** were examined by ^{1}H NMR spectroscopy.[11] Spectral changes upon addition of **G1** to a solution of **1** in $CDCl_3$ are shown in Figure 1. Precise addition of **G1** of up to two equivalents caused the appearance of a new set of sharp signals at the expense of those of free **1** (Figure 1 a–c), thus indicating the formation of the **1**–**G1** complex in a stoichiometric ratio of

Abstract in Japanese:
ビピリジル類縁体をゲスト分子として用いることでポルフィリンシート1が2：4対面型ダイマーを形成した。これら複合体の^{1}H NMR から、1の空間的な誘起磁場効果を実験的に明らかにし、NICS を用いた理論計算によってもこれを検討した。

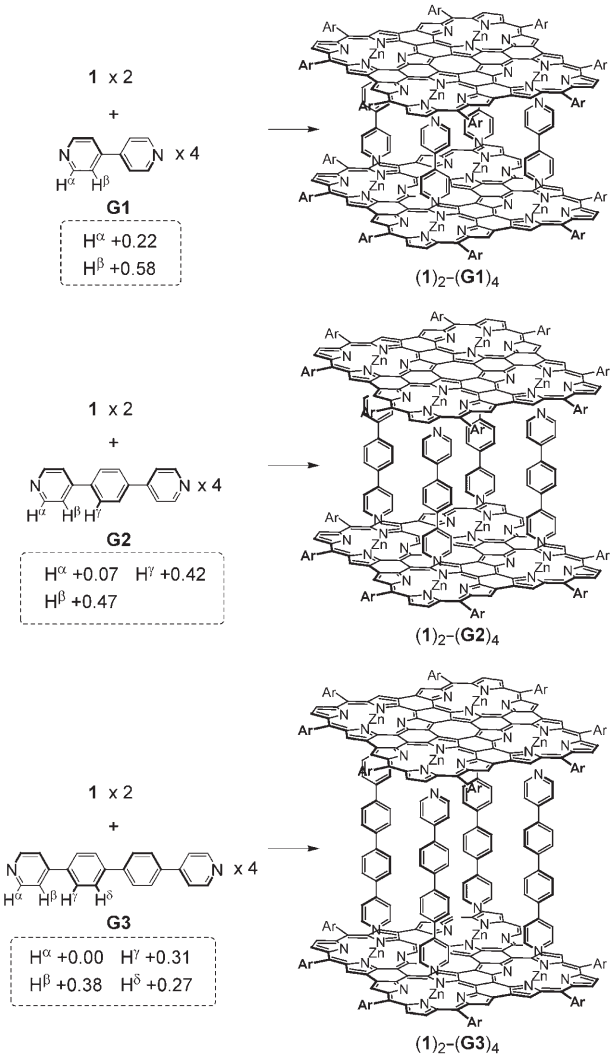

Scheme 2. Formation of dimeric complexes, and the CIS values in ppm.

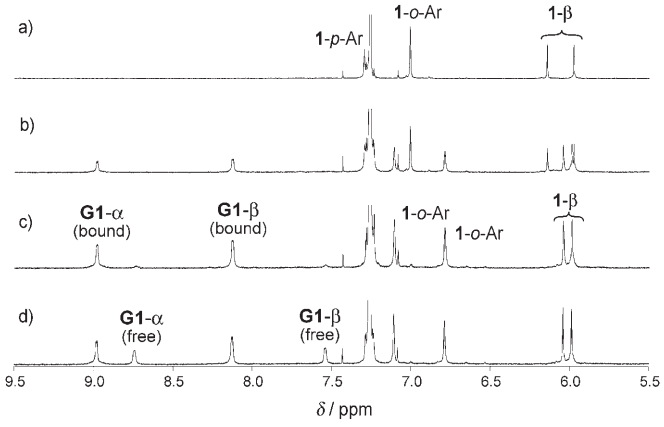

Figure 1. ^{1}H NMR spectra of **1** (1×10^{-7} M) with a) 0, b) 1, c) 2, d) 3 equivalents of **G1** in $CDCl_3$ containing *n*-butylamine ($\approx8\times10^{-7}$ M).

1:2. This stoichiometry of complexation was also confirmed by the Job plot (see Supporting Information). At the exact ratio **G1**/**1** = 2, the spectrum became simple (Figure 1c); the compound here was assigned as the 2:4 face-to-face type II complex $(\mathbf{1})_2$–$(\mathbf{G1})_4$ on the basis of its high symmetry (D_{4h}) and the signal-intensity ratios (Scheme 2).

For the assignment of the ^{1}H NMR spectrum of $(\mathbf{1})_2$–$(\mathbf{G1})_4$, partially α-deuterated 4,4′-bipyridyl ($[D_\alpha]\mathbf{G1}$; ≈50%) was prepared and complexed with **1** (see Supporting Information).[12] The ^{1}H NMR chemical shifts of $(\mathbf{1})_2$–$([D_\alpha]\mathbf{G1})_4$ are identical to those of $(\mathbf{1})_2$–$(\mathbf{G1})_4$, thus indicating the formation of the same face-to-face dimeric complex. Comparison of the signal intensities of the pyridyl protons in these two complexes revealed that the peaks at 8.93 and 8.13 ppm are due to the α and β protons, respectively. All the signals were thus assigned as shown in Figure 1.

The observed simple peaks for guest protons indicate that the bipyridine-type guest molecules undergo free rotation within the complexes even at −60 °C, as confirmed by variable-temperature NMR spectroscopy. Notably, the signals of the *para* protons of the *meso*-aryl group of **1** in $CDCl_3$ were hidden by a solvent peak. Therefore, to confirm the signals of *para*-aryl protons, [D$_2$]tetrachloroethane was used for ^{1}H NMR spectroscopy (see Supporting Information). Although the signals of the pyrrole β protons of the porphyrin sheet were now unfortunately covered by a solvent peak, the signals of the *para*-aryl protons were observed.[13] All the peak assignments were performed with 2D NMR spectroscopy. In accord with this assignment, the signals of the *ortho* protons of the *meso*-aryl groups were observed as split signals, which reflects their different locations, either inside or outside the complex $(\mathbf{1})_2$–$(\mathbf{G1})_4$; this proved its sandwich conformation. Further addition of **G1** led to the appearance of a set of signals due to free **G1** (Figure 1d), and any dissociation of $(\mathbf{1})_2$–$(\mathbf{G1})_4$ was not detected even after addition of another 10 equivalents of **G1**. Here, the peaks for free **G1** appeared at 8.74 and 7.54 ppm, thus confirming the apparent downfield shifts of the pyridyl protons of the bound **G1**. During these titration experiments, no other peaks due to partially bound species were detected, which indicates that the binding of **G1** with **1** is strongly allosteric, and the formation of the complex $(\mathbf{1})_2$–$(\mathbf{G1})_4$ is an all-or-nothing process.[14]

Similar binding experiments with elongated guest molecules **G2** and **G3** showed similar 2:4 complexation behavior, although the binding of **G3** to **1** was weaker and in competition with *n*-butylamine.[15] Precise addition of 2 equivalents of **G2** also caused the appearance of a new set of sharp signals, which was assigned to the 2:4 face-to-face complex $(\mathbf{1})_2$–$(\mathbf{G2})_4$ for the same reason as for $(\mathbf{1})_2$–$(\mathbf{G1})_4$ (Scheme 1). Assignments of the guest signals in $(\mathbf{1})_2$–$(\mathbf{G2})_4$ and $(\mathbf{1})_2$–$(\mathbf{G3})_4$ were performed on the basis of the 2D ^{1}H-^{1}H NOESY spectrum, which revealed the correlation between the pyridyl β protons (H^β) and the 1,4-phenylene protons (H^γ) (Figures 2 and 3). The peaks for bound **G2** appeared at 8.77 (H^α), 8.20 (H^γ), and 8.03 ppm (H^β), whereas those for free **G2** appeared at 8.71 (H^α), 7.78 (H^γ), and 7.56 ppm

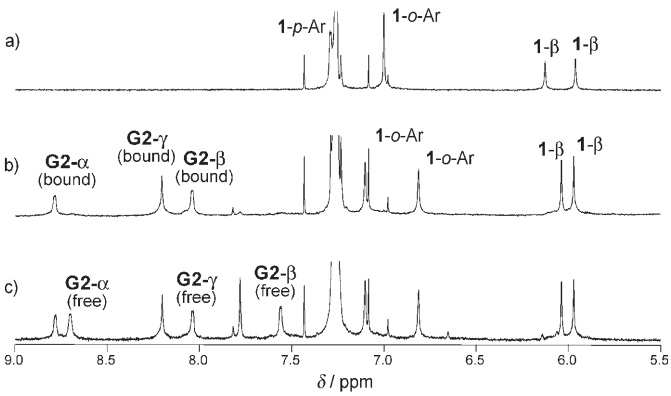

Figure 2. ^{1}H NMR spectra of **1** (1×10^{-7} M) with a) 0, b) 2, and c) 4 equivalents of **G2** in $CDCl_3$ containing *n*-butylamine (≈8×10^{-7} M).

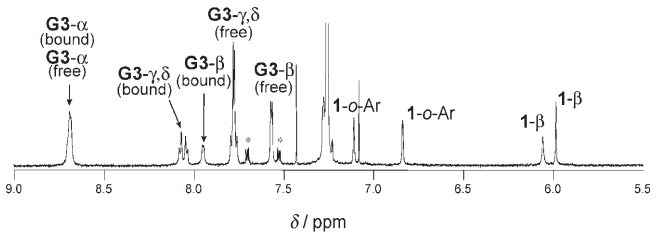

Figure 3. ^{1}H NMR spectrum of **1** with an excess of **G3** in $CDCl_3$. Impurities are indicated by *.

(H^β). The peaks for bound **G3** appeared at 8.69 (H^α), 8.08 (H^γ), 8.04 (H^δ), and 7.95 ppm (H^β), whereas those for free **G3** appeared at 8.70 (H^α), 7.77 (H^γ and H^δ), and 7.57 ppm (H^β).

The guest molecules **G1**–**G3** are linear and thus pertinent for the examination of distance (vertical) dependence of the induced magnetic effects of **1**. In these complexes, we have to consider the magnetic influences of the two porphyrin sheets, because the guest molecules are sandwiched between them.

Changes in chemical shift arising from guest binding, that is, complexation-induced shifts (CIS; $\Delta\delta = \delta_{bound} - \delta_{free}$), have been extensively used to assign structures in solution qualitatively.[16] The use of CIS values simplifies the problem because through-bond effects are eliminated. The CIS values of **G1**–**G3** are given in Scheme 2. The CIS values of the pyridyl protons of the guest molecules are quite different from the general upfield shifts of pyridine bound to zinc porphyrins ($\Delta\delta \approx -6.0$ ppm for α protons, $\Delta\delta \approx -1.8$ ppm for β protons).[5a,17]

Notably, the CIS values for the pyridyl α protons decreased in the order **G1** (+0.23) > **G2** (+0.07) > **G3** (0.00 ppm). Given that the magnetic influence of the proximal porphyrin sheet toward the pyridyl α protons, which possibly includes the shielding effect of the local porphyrin moiety and the deshielding effect of the overall porphyrin sheet, are the same in the series, the observed systematic changes in the CIS values imply the differing magnetic influence of the remote porphyrin sheet. In other words, the de-

CHEMISTRY
AN ASIAN JOURNAL

shielding influence of the remote porphyrin sheet decreases in the order **G1** > **G2** > **G3**. Another important observation is that the pyridyl β protons exhibited the largest downfield shifts in these three complexes, and such downfield shifts are attenuated for the γ and δ protons. It is therefore interesting that the distance profile of the CIS value has a saddle point in these face-to-face complexes.

Furthermore, we investigated the paratropic ring-current effect just above the COT core by using **G4** to make a type I complex. The distance between the two nitrogen atoms of the pyridine moiety of **G4** was estimated to match the distance between the diagonal zinc(II) ions in **1** well. The complex of **1** with **G4** was prepared by using a similar procedure to the preparation of **1**–(**2**)$_2$. An excess of **G4** was added to a solution of **1** in $CHCl_3$ followed by dilution of the solution with acetonitrile. The resulting solution was slowly evaporated to form the precipitate of the complex. Although the ^{1}H NMR spectrum of **1** with **G4** in $CDCl_3$ at room temperature (20 °C) showed the formation of the complex, as indicated by the disappearing of the original peaks of **1**, the signals of **G4** were hardly observed. Clear signals of both **1** and **G4** in the complex were obtained in the NMR spectrum at −25 °C, and the stoichiometry of the complex was determined by signal-intensity ratios to be 1:2, thus indicating the complex **1**–**(G4)**$_2$ (Scheme 3). The assignment of

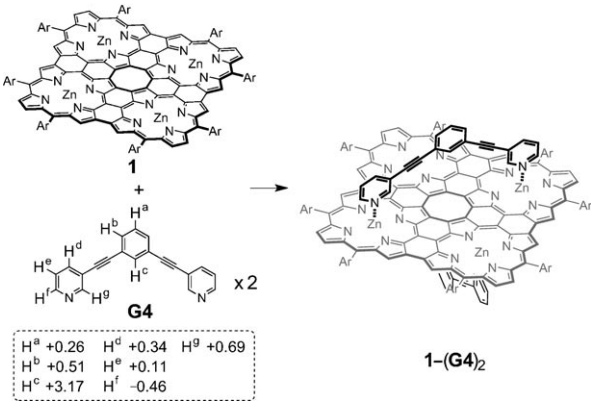

Scheme 3. Formation of the complex of **1** and **G4**, and the CIS values in ppm.

the signals shown in Figure 4 was performed on the basis of the 2D COSY spectrum. The signals of the phenylene protons of bound **G4** appeared at 7.40 (H^a), 7.54 (H^b), and 7.75 ppm (H^c), and those of the pyridyl protons were observed at 8.17 (H^d), 7.44 (H^e), 8.11 (H^f), and 9.46 ppm (H^g).

Complex **1**–(**G4**)$_2$ gives us useful information about the ring-current effect, because the protons in **G4** are located in the wide area above the porphyrin sheet. The respective negative and positive CIS values of the pyridyl protons H^f and H^g indicate that the induced magnetic field far from the COT core is diatropic, whereas that near it is paratropic. The opposite signs of the CIS values for H^e and H^f indicate that the induced magnetic effect above the zinc atom

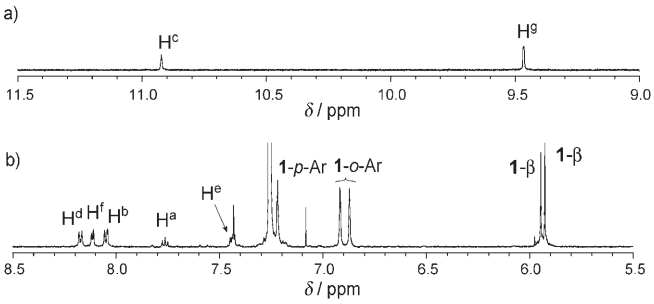

Figure 4. ^{1}H NMR spectra of **1**–(**G4**)$_2$ in $CDCl_3$ at −25 °C. a) Low-field region. b) High-field region.

changes from an upfield to a downfield shift with distance from the plane. The order of CIS of the central phenylene protons of **G4** is H^c (+3.17) > H^b (+0.51) > H^a (+0.26 ppm), which corresponds to the order of the distances of these protons from the plane of **1.**

Theoretical Studies

In the previous report, we showed that **1** exhibits a deshielding magnetic effect above the COT core, but that the local porphyrin subunits retain a weak shielding effect.[8] As a consequence of these opposing effects, small upfield shifts were observed above the zinc(II) porphyrin moieties in **1**. The present observations may be accounted for in terms of the following induced-magnetic-field model: 1) the magnetic field above the zinc(II) ion is diatropic where the paratropic magnetic effects due to the COT core is weak; 2) a weaker diatropic magnetic effect for the bound pyridyl α protons is expected because of free rotation of the bipyridyl-type guest molecules in the complex, by which the pyridyl α protons experience paratropic magnetic effects due to the COT core; 3) with an increase in the distance from the plane, the diatropic magnetic field of the porphyrin subunit is decreased and is overwhelmed at a certain point by the paratropic magnetic field of the COT core; 4) a further increase in the distance causes a decrease in the paratropic field; and 5) the shielding and deshielding magnetic influences of the two porphyrin sheets in **1** behave independently.

First, we calculated the distance dependence of the nucleus-independent chemical shift (NICS) values of monomeric **1** to gain insight into the magnetic field above the porphyrin sheet.[18] *Meso*-unsubstituted (*meso*-H) porphyrin sheet **1**H was used for geometry optimization and NMR calculations. The optimized structure obtained was completely planar. The NICS probes (Bq atoms) were placed above the geometric center of the COT core and at selected points (above the zinc atoms and above eight points along the zinc-ion-centered circle of radius 2 Å, as the bipyridine-type guest molecules undergo free rotation within the complexes, and the distance between its central molecular axis and the hydrogen atoms are estimated to be about 2 Å) at distances ranging from 0.0 (i.e., in the molecular plane) to 20.0 Å at 0.5-Å steps along the line perpendicular to the molecular

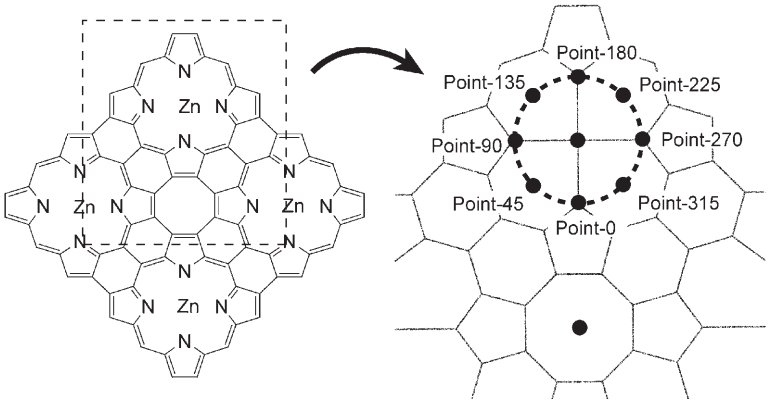

Scheme 4. Filled circle: position of Bq atom. Dotted circle: Zn-ion-centered circle of radius 2 Å. One point along the circle was placed on the Zn–COT center line (this point is defined as point-0), and the other points are placed in a clockwise manner at 45° steps from this point (point-45 to point-315).

plane (Scheme 4).[19] As shown in a previous report of the distance-dependent NICS plot of cyclobutadiene,[18b] a typical antiaromatic molecule, the NICS at the center of the COT core decreases monotonously with increasing distance (Figure 5). In the complex **1**–(**G4**)$_2$, H^a and H^c are above the geometric center of the COT core, and the distances of H^a and H^c to the plane of **1** were estimated to be 9.8 and 4.8 Å, respectively. The CIS values of these protons (H^a = 0.26, H^c = 3.17 ppm) coincide with the calculated NICS values (0.41–0.35 ppm for 9.5–10-Å and 4.2–3.1 ppm for 4.5–5-Å distances).

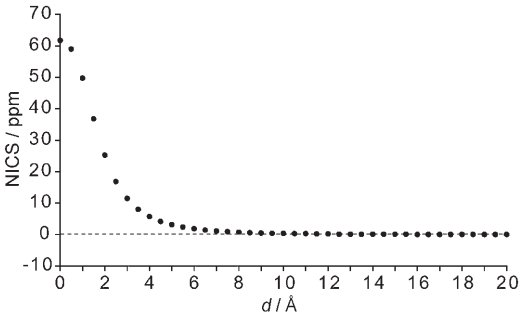

Figure 5. Plot of NICS values up to 20 Å from the geometric center of COT.

Figure 6a shows the difference in NICS among the points along the circle. The points along the zinc-ion-centered circle are shown in Scheme 4. At points close to the COT core, such as point-0, -45, and -315, the magnetic effect is almost wholly (distance > 3 Å) deshielding, and the maximum positive NICS is at 4–6 Å. On the other hand, at points far from COT, such as point-135, -180, and -225, the NICS is negative throughout the varying distances. These results indicate that the deshielding magnetic effect is predominant in the region close to the central COT but weak away from it. Although the reason for the positive CIS for H^e is not clear at this time, these results agree well with the experimental positive and negative CIS values for H^g and H^f of **G4**, whose positions correspond to point-0 and point-180, respectively. Figure 6b and c shows that the distance-dependent NICS values at the zinc ion and the averaged NICS values of the points along the circle (NICS$_{eff}$) are very similar. The NICS$_{eff}$ value is negative close to the plane of the porphyrin sheet and increases steeply to reach the largest value of about 0.09 ppm at 7.5 Å; it then decreases gradually with increasing separation from the plane.

Next, we estimated the magnetic influences that the bound

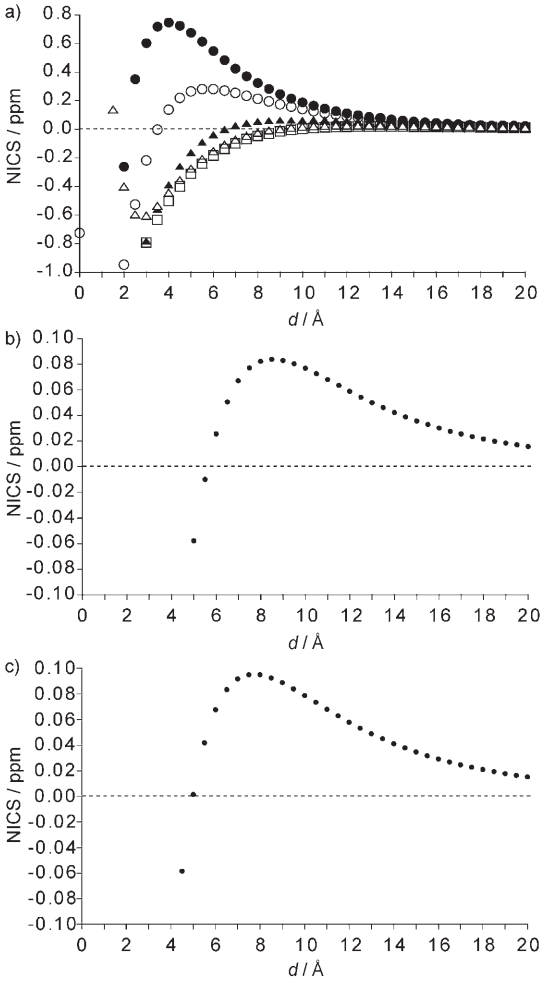

Figure 6. Plots of NICS values a) at the points on the dotted circle in Scheme 4: ● = point-0, ○ = point-45, ▲ = point-90, △ = point-135, □ = point-180 (the values at point-225, -270, and -315 were the same as those at point-135, -90, and -45, respectively), b) at the zinc atom, and c) averaged among the eight points on the circle.

CHEMISTRY
AN ASIAN JOURNAL

guest molecule experiences within the 2:4 complexes by setting the separations between the porphyrin sheets as 11.5 Å for $(\mathbf{1})_2$–$(\mathbf{G1})_4$, 16.0 Å for $(\mathbf{1})_2$–$(\mathbf{G2})_4$, and 20.5 Å for $(\mathbf{1})_2$–$(\mathbf{G3})_4$, in which the distances are based on the calculated molecular length of the guest molecules and general N–Zn distances in pyridine–Zn^{II} porphyrin complexes.

The distance profiles of the NICS values thus estimated are shown in Figure 7 b–d. Whereas a simple bell-type profile was estimated for the complex $(\mathbf{1})_2$–$(\mathbf{G1})_4$, the peak

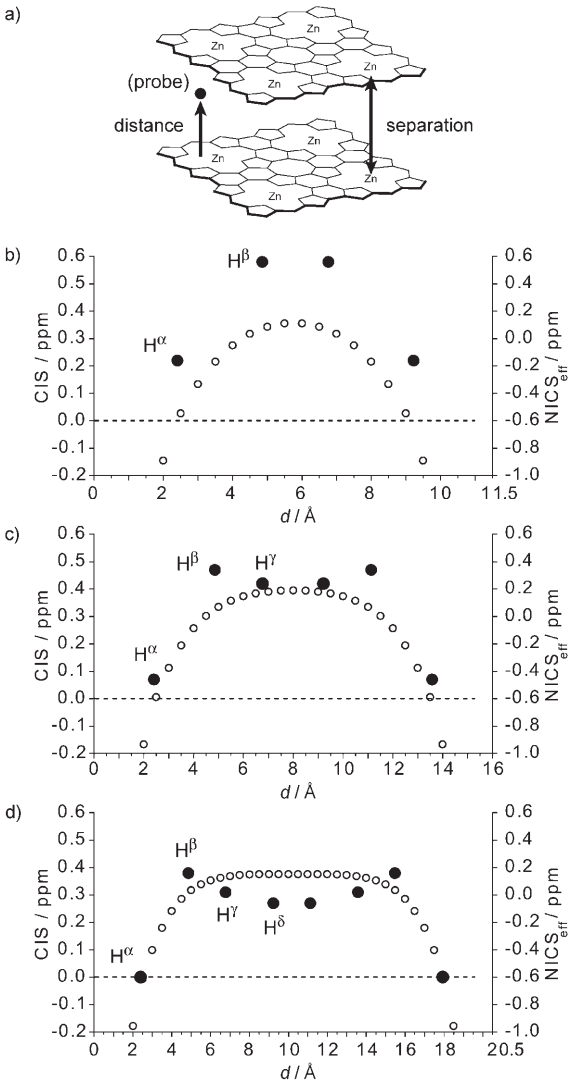

Figure 7. a) Face-to-face dimer model. b–d) Plots of $NICS_{eff}$ values of dimeric **1** at a separation of 11.5 (b), 16.0 (c), and 20.5 Å (d) from COT. Experimental CIS values of $(\mathbf{1})_2$–$(\mathbf{G1})_4$, $(\mathbf{1})_2$–$(\mathbf{G2})_4$, and $(\mathbf{1})_2$–$(\mathbf{G3})_4$ are plotted in b), c), and d), respectively. ○ = $NICS_{eff}$, ● = CIS.

shape of the distance profiles gradually became flat for $(\mathbf{1})_2$–$(\mathbf{G2})_4$ and $(\mathbf{1})_2$–$(\mathbf{G3})_4$. The present model explains the observed larger deshielding influence at the pyridyl β protons relative to that of the pyridyl α protons, but contradicts the smaller deshielding influence at the pyridyl γ protons relative to that of the pyridyl β protons. At present, we believe that these discrepancies between the distance dependence of the observed CIS and calculated NICS values derive from the dynamic motion and the deformation of the complexes. The calculated structures were completely flat and the two porphyrin sheets overlapped perfectly, whereas, in reality, the coordination of pyridyl ligands to zinc atoms deforms the porphyrin sheet, and the two sheets can sway along with four bipyridyl guest molecules in solution. This may cause the ^{1}H NMR signals of the pyridyl protons to be shifted downfield.

Conclusions

The distance dependence of the induced magnetic effect is becoming more important in understanding the ring current of conjugated aromatic and antiaromatic circuits.[20] In this respect, the porphyrin sheet **1** is an intriguing host that exhibits both deshielding and shielding magnetic influences with different magnitudes and distance profiles. Thus, the use of pyridine-based guest molecules of various shapes and molecular lengths provides a rare opportunity for the examination of the spatial dependence of the induced magnetic effect.

Experimental Section

General Procedures

All reagents and solvents were of commercial reagent grade and were used without further purification. ^{1}H NMR spectra were recorded on a JEOL ECA-delta-600 spectrometer at room temperature unless otherwise noted, and chemical shifts are reported in ppm relative to $CHCl_3$ ($\delta = 7.26$ ppm) or tetrachloroethane ($\delta = 5.91$ ppm). Preparative separations were performed by silica-gel column chromatography (Wako gel C-300) under gravity. All calculations were performed with the Gaussian 03 program.[21] *Meso*-unsubstituted (*meso*-H) porphyrin sheet **1**H was used for geometry optimization and NMR calculations. Geometries were optimized by using the B3LYP DFT method with the LANL2DZ basis set for the zinc atom and the 6-31G* basis set for the other atoms (denoted as 631LAN) without any symmetry restriction.[22] NICS values were computed at the GIAO-B3LYP/631LAN//B3LYP/631LAN level.

Syntheses

G2 and **G3**: 1,4-Di(4-pyridyl)benzene (**G2**) and 4,4′-di(4-pyridyl)biphenyl (**G3**) were synthesized by palladium-catalyzed coupling of (4-pyridyl)boronic acid pinacol ester with 1,4-dibromobenzene and 4,4′-dibromobiphenyl, respectively. **G2**: ^{1}H NMR ($CDCl_3$): $\delta = 8.71$ (d, $J = 5.1$ Hz, 4H, py), 7.78 (s, 4H, Ph), 7.56 ppm (d, $J = 5.3$ Hz, 4H, py). **G3**: ^{1}H NMR ($CDCl_3$): $\delta = 8.70$ (d, $J = 6$ Hz, 4H, py), 7.78–7.76 (m, 8H, Ph), 7.57 ppm (d, $J = 5.9$ Hz, 4H, py).

G4: 1,3-Bis(4-pyridylethynyl)benzene (**G4**) was synthesized by following the published procedure. ^{1}H NMR ($CDCl_3$, −25 °C) $\delta = 8.77$ (s, 2H, py), 8.57 (d, $J = 4.8$ Hz, 2H, py), 7.83 (d, $J = 7.9$ Hz, 2H, py), 7.75 (s, 1H, Ph), 7.54 (d, $J = 4.6$ Hz, 2H, Ph), 7.40 (t, $J = 7.7$ Hz, 1H, Ph), 7.35–7.31 (m, 2H, py).

Complexation Experiments

For **G1** and **G2**, a solution of guest (1×10^{-2} M) in $CDCl_3$ or [D_2]tetrachloroethane containing *n*-butylamine ($\approx 8 \times 10^{-7}$ M) was added stepwise to a solution of **1** (1×10^{-7} M, 0.5 mL) in the same deuterated solvent. For **G3**, a solution of **G3** in $CHCl_3$ was added to a solution of **1** (5×

10^{-8} M) in $CHCl_3$ and butylamine ($\approx 4\times10^{-7}$ M, 1 mL). The solvent was then evaporated, and $CDCl_3$ was added to the residue. The complexation procedure for **G4** is described in the text.

(**1**)$_2$–(**G1**)$_4$: ^{1}H NMR ($CDCl_3$): $\delta = 8.98$ (s, 16H, **G1**), 8.13 (s, 16H, **G1**), 7.11 (s, 16H, **1**-Ar), 6.79 (s, 16H, **1**-Ar), 6.04 (s, 16H, **1**-β), 5.99 (s, 16H, **1**-β), 1.24 (s, 144H, **1**-*t*Bu), 1.11 ppm (s, 144H, 1-*t*Bu); ^{1}H NMR ([D$_2$]tetrachloroethane): $\delta = 9.01$ (s, 16H, **G1**), 8.19 (s, 16H, **G1**), 7.17 (s, 16H, **1**-Ar), 7.00 (s, 16H, **1**-Ar), 6.71 (s, 16H, **1**-Ar), 1.17 (s, 144H, **1**-*t*Bu), 1.14 ppm (s, 144H, **1**-*t*Bu) ppm. The **1**-*p*-Ar peak in $CDCl_3$ and **1**-β peaks in [D$_2$]tetrachloroethane were hidden by the large solvent peak.

(**1**)$_2$–(**G2**)$_4$: ^{1}H NMR ($CDCl_3$): $\delta = 8.77$ (s, 16H, **G2**), 8.20 (s, 16H, **G2**), 8.03 (s, 16H, **G2**), 7.10 (s, 16H, **1**-Ar), 6.81 (s, 16H, **1**-Ar), 6.04 (s, 16H, **1**-β), 5.97 (s, 16H, **1**-β), 1.25 (s, 144H, **1**-*t*Bu), 1.15 ppm (s, 144H, **1**-*t*Bu).

(**1**)$_2$–(**G3**)$_4$: ^{1}H NMR ($CDCl_3$): $\delta = 8.69$ (s, 16H, **G3**), 8.08 (d, $J = 7.2$ Hz, 16H, **G3**), 8.04 (d, $J = 7.6$ Hz, 16H, **G3**), 7.95 (s, 16H, **G3**), 7.11 (s, 16H, **1**-Ar), 6.84 (s, 16H, **1**-Ar), 6.06 (s, 16H, **1**-β), 5.99 (s, 16H, **1**-β), 1.25 (s, 144H, **1**-*t*Bu), 1.17 ppm (s, 144H, **1**-*t*Bu).

1–(**G4**)$_2$: ^{1}H NMR ($CDCl_3$, −25 °C): $\delta = 10.92$ (s, 2H, **G4**), 9.46 (s, 4H, **G4**), 8.17 (d, $J = 7.8$ Hz, 4H, **G4**), 8.11 (d, $J = 3.7$ Hz, 4H, **G4**), 8.05 (d, $J = 9.2$ Hz, 4H, **G4**), 7.76 (t, $J = 7.8$ Hz, 2H, **G4**), 7.45–7.42 (m, 4H, **G4**), 7.22 (s, 8H, **1**-Ar), 6.92 (s, 8H, **1**-Ar), 6.87 (s, 8H, **1**-Ar), 5.95 (s, 8H, **1**-β), 5.93 (s, 8H, **1**-β), 1.17 (s, 144H, **1**-*t*Bu), 1.13 ppm (s, 144H, **1**-*t*Bu).

Acknowledgements

This work was partly supported by a Grant-in-Aid for Scientific Research (B) (No.17350017) from the Ministry of Education, Culture, Sports, Science, and Technology, Japan and the 21st Century COE on Kyoto University Alliance for Chemistry. Y.N. thanks the JSPS Research Fellowship for Young Scientists.

[1] E. R. P. Zuiderweg, *Biochemistry* **2002**, *41*, 1.
[2] a) M. P. Williamson, T. F. Havel, K. Wüthrich, *J. Mol. Biol.* **1985**, *182*, 295; b) K. Wüthrich, *Nat. Struct. Biol.* **2001**, *8*, 923.
[3] C. A. Hunter, M. J. Packer, C. Zonta, *Prog. Nucl. Magn. Reson. Spectrosc.* **2005**, *47*, 27.
[4] M. Gouterman in *The Porphyrins*, *Vol. III* (Ed.: D. Dolphin), Academic Press, New York, **1979**, p. 87.
[5] a) J. K. M. Sanders in *The Porphyrin Handbook*, *Vol. 3* (Eds.: K. M. Kadish, K. M. Smith, R. Guilard), Academic Press, San Diego, **2000**, p. 347; b) A. Tsuda, T. Nakamura, S. Sakamoto, K. Yamaguchi, A. Osuka, *Angew. Chem.* **2002**, *114*, 2941; *Angew. Chem. Int. Ed.* **2002**, *41*, 2817; c) I.-W. Hwang, T. Kamada, T. K. Ahn, D. M. Ko, T. Nakamura, A. Tsuda, A. Osuka, D. Kim, *J. Am. Chem. Soc.* **2004**, *126*, 16187.
[6] a) R. J. Abraham, S. C. M. Fell, K. M. Smith, *Org. Magn. Reson.* **1977**, *9*, 367; b) R. J. Abraham, G. R. Bedford, D. McNeillie, B. Wright, *Org. Magn. Reson.* **1980**, *14*, 418.
[7] Examples of antiaromatic porphyrinoids: a) J. L. Sessler, S. J. Weghorn, Y. Hisaeda, V. Lynch, *Chem. Eur. J.* **1995**, *1*, 56; b) C.-H. Hung, J.-P. Jong, M.-Y. Ho, G.-H. Lee, S.-M. Peng, *Chem. Eur. J.* **2002**, *8*, 4542; c) S. Mori, J.-Y. Shin, S. Shimizu, F. Ishikawa, H. Furuta, A. Osuka, *Chem. Eur. J.* **2005**, *11*, 2417; d) S. Mori, A. Osuka, *J. Am. Chem. Soc.* **2005**, *127*, 8030; e) J. A. Cissell, T. P. Vaid, A. L. Rheingold, *J. Am. Chem. Soc.* **2005**, *127*, 12212; f) Y. Yamamoto, A. Yamamoto, S.-y. Furuta, M. Horie, M. Kodama, W. Sato, K.-y. Akiba, S. Tsuzuki, T. Uchimaru, D. Hashizume, F. Iwasaki, *J. Am. Chem. Soc.* **2005**, *127*, 14540.
[8] Y. Nakamura, N. Aratani, H. Shinokubo, A. Takagi, T. Kawai, T. Matsumoto, Z. S. Yoon, D. Y. Kim, T. K. Ahn, D. Kim, A. Muranaka, N. Kobayashi, A. Osuka, *J. Am. Chem. Soc.* **2006**, *128*, 4119.
[9] a) K. Biradha, M. Fujita, *J. Chem. Soc. Dalton Trans.* **2000**, 3805; b) K. Biradha, Y. Hongo, M. Fujita, *Angew. Chem.* **2000**, *112*, 4001; *Angew. Chem. Int. Ed.* **2000**, *39*, 3843.
[10] N. Schultheiss, J. M. Ellsworth, E. Bosch, C. L. Barnes, *Eur. J. Inorg. Chem.* **2005**, 45.
[11] A titration experiment with absorption spectroscopy did not succeed because of only small spectral changes upon complexation.
[12] In our hands, all α-deuterated compounds could not be synthesized; see: W. R. Browne, C. M. O'Connor, J. S. Killeen, A. L. Guckian, M. Burke, P. James, M. Burke, J. G. Vos, *Inorg. Chem.* **2002**, *41*, 4245.
[13] [D$_2$]Dichloromethane or [D$_6$]benzene is possibly more suitable for ^{1}H NMR spectroscopy of **1** than [D$_2$]tetrachloroethane as they do not produce peaks that overlap with any of the peaks of **1** and the guest molecules. However, these solvents did not give clear spectra mainly due to low solubility.
[14] P. N. Taylor, H. L. Anderson, *J. Am. Chem. Soc.* **1999**, *121*, 11538.
[15] Therefore, in the case of (**1**)$_2$–(**G3**)$_4$, butylamine was removed under reduced pressure after the addition of **G3** to complete the complexation.
[16] a) C. A. Hunter, *J. Am. Chem. Soc.* **1992**, *114*, 5303; b) X. Chi, A. J. Guerin, R. A. Haycock, C. A. Hunter, L. D. Sarson, *J. Chem. Soc. Chem. Commun.* **1995**, 2567.
[17] A similar assembly of a fused porphyrin dimer was reported, for which the bound bipyridyl protons showed a negative CIS: a) H. Sato, K. Tashiro, H. Shinmori, A. Osuka, T. Aida, *Chem. Commun.* **2005**, 2324; b) H. Sato, K. Tashiro, H. Shinmori, A. Osuka, Y. Murata, K. Komatsu, T. Aida, *J. Am. Chem. Soc.* **2005**, *127*, 13086.
[18] a) Z. Chen, C. S. Wannere, C. Corminboeuf, R. Puchta, P. von R. Schleyer, *Chem. Rev.* **2005**, *105*, 3842; b) P. von R. Schleyer, M. Manoharan, Z.-X. Wang, B. Kiran, H. Jiao, R. Puchta, N. J. R. van Eikema Hommes, *Org. Lett.* **2001**, *3*, 2465; c) A. Stanger, *J. Org. Chem.* **2006**, *71*, 883.
[19] In the calculations, very large positive or negative NICS values were found at the points that are very close to an atom or a bond. Therefore, for some probes, especially at the zinc ion, point-0, -90, -180, and -270, NICS values are not useful in the small-distance region; see reference [18c].
[20] Direct mapping of the ring current of porphyrinoids and COT derivatives were recently developed: a) E. Steiner, P. W. Fowler, *ChemPhysChem* **2002**, *3*, 114; b) E. Steiner, P. W. Fowler, *Org. Biomol. Chem.* **2003**, *1*, 1785; c) E. Steiner, P. W. Fowler, *Org. Biomol. Chem.* **2004**, *2*, 34; d) P. W. Fowler, R. W. A. Havenith, L. W. Jenneskens, A. Soncini, E. Steiner, *Angew. Chem.* **2002**, *114*, 1628; *Angew. Chem. Int. Ed.* **2002**, *41*, 1558.
[21] M. J. Frisch, G. W. Trucks, H. B. Schlegel, G. E. Scuseria, M. A. Robb, J. R. Cheeseman, J. A. Montgomery, Jr., T. Vreven, K. N. Kudin, J. C. Burant, J. M. Millam, S. S. Iyengar, J. Tomasi, V. Barone, B. Mennucci, M. Cossi, G. Scalmani, N. Rega, G. A. Petersson, H. Nakatsuji, M. Hada, M. Ehara, K. Toyota, R. Fukuda, J. Hasegawa, M. Ishida, T. Nakajima, Y. Honda, O. Kitao, H. Nakai, M. Klene, X. Li, J. E. Knox, H. P. Hratchian, J. B. Cross, C. Adamo, J. Jaramillo, R. Gomperts, R. E. Stratmann, O. Yazyev, A. J. Austin, R. Cammi, C. Pomelli, J. W. Ochterski, P. Y. Ayala, K. Morokuma, G. A. Voth, P. Salvador, J. J. Dannenberg, V. G. Zakrzewski, S. Dapprich, A. D. Daniels, M. C. Strain, O. Farkas, D. K. Malick, A. D. Rabuck, K. Raghavachari, J. B. Foresman, J. V. Ortiz, Q. Cui, A. G. Baboul, S. Clifford, J. Cioslowski, B. B. Stefanov, G. Liu, A. Liashenko, P. Piskorz, I. Komaromi, R. L. Martin, D. J. Fox, T. Keith, M. A. Al-Laham, C. Y. Peng, A. Nanayakkara, M. Challacombe, P. M. W. Gill, B. Johnson, W. Chen, M. W. Wong, C. Gonzalez, J. A. Pople, Gaussian 03, Revision B.05, Gaussian, Inc., Pittsburgh, PA (USA), **2003**.
[22] a) A. D. Becke, *Phys. Rev. A* **1988**, *38*, 3098; b) C. Lee, W. Yang, R. G. Parr, *Phys. Rev. B* **1988**, *37*, 785.

Received: April 3, 2007
Published online: June 13, 2007

